A new synthesis route to produce isocyanate-free polyurethane foams

Clara Amezúa-Arranz [a,*], Mercedes Santiago-Calvo [a], Miguel-Ángel Rodríguez-Pérez [a,b]

[a] *Cellular Materials Laboratory (CellMat), Condensed Matter Physics Department, Faculty of Science, University of Valladolid, Campus Miguel Delibes, Paseo de Belén 7, 47011 Valladolid, Spain*
[b] *BioEcoUVA Research Institute on Bioeconomy, University of Valladolid, Spain*

ARTICLE INFO

ABSTRACT

Isocyanate is a toxic substance that is one of the main reactants used in the conventional fabrication route for polyurethane foams. This study presents the synthesis of isocyanate-free polyurethane foams from cyclic carbonates and diamines using sodium bicarbonate as the foaming agent. Three different series of foams are synthesised using three types of sodium bicarbonates having different average particle sizes (i.e. 3, 13, and 22 μm) at four content levels (i.e. 5, 10, 15, and 20 wt% with respect to cyclic carbonate). The density, open-cell content, average cell size, normalised standard deviation of the cell size distribution, anisotropy, cell density and cell nucleation density are characterized for all the materials synthesized. In addition, a theoretical study of the expected densities is conducted to compare the theoretical values with the experimental densities obtained for the foams. Finally, the foams previously manufactured with high sodium-bicarbonate content are optimised by modifying the catalyst content from 0.5 to 2.0 wt% with respect to cyclic carbonate, thereby producing foams with lower densities. Nonisocyanate polyurethane foams having densities as low as 142 kg/m^3 are fabricated.

1. Introduction

Polyurethane (PUs), invented by Otto Bayer in 1937 [1], is one of the most versatile polymers with a unique combination of properties that allow its application in a wide range of different industrial sectors, such as automotive, construction, furniture, packaging, medicine, and sports. Because of the various PU synthesis methods, different types of PU materials are available, including flexible foams for comfort and wellness (e.g. bed mattresses and furniture); foams for acoustic absorption, filtering, or shock absorption in the automation sector, rigid foams used in thermal or acoustic insulation; elastomer fibres for textiles; and solid elastomers for shoes and components of adhesives and sealants. In addition, thermoset PU foams cover most of the PU market and are among the largest segments of the polymeric foam market, representing more than 50% of the global foam market [2].

Industrially, the synthesis of PU foams is primarily based on two simultaneous reactions: the polymerisation or gelling reaction, in which isocyanate reacts with a polyol to create a PU matrix, and the foaming or blowing reaction, in which gas is generated to expand the foam by adding physical or chemical blowing agents [3]. Physical blowing agents are typically liquids having low boiling points, such as hydro-carbons or hydrofluoroolefins, which volatilise during exothermic foaming. Chemical blowing agents, such as water, produce gas via chemical reactions. Water is the most commonly used blowing agent in several PU foam applications. In water-blown PU foams, isocyanate reacts with water to form unstable carbamic acid, which spontaneously decomposes into CO_2 and its corresponding amine. Subsequently, the generated amine continues to react with isocyanate to generate urea products. Therefore, polyols, isocyanates, and water are the most critical starting components for the synthesis of PU foams having complex structures.

Most isocyanates and polyols used in the PU industry are produced from petroleum-based ingredients [4], which are non-renewable resources with substantial drawbacks. Thus, the petroleum crisis and environmental concerns have increased the need for more suitable and environmentally friendly alternatives to replace petroleum-based PU components. As such, academic and industrial attention has been recently focused on replacing all or some of the conventional petroleum-based polyols with polyols from renewable resources, such as biomass residues, vegetable oils, or industrial by-products [5]. However, PU foams containing biopolyols must be produced using isocyanate because only few compounds can replace this reaction. The most important commercial method for isocyanate production based on the phosgenation of amines presents a considerable health problem, as exposure to

---

phosgene, which is a highly toxic gas, can cause severe respiratory effects, ocular irritation, burns to the eye and skin, and eventually death [6]. Moreover, the obtained isocyanate monomers are harmful compounds [6,7]. Consequently, several studies are being conducted with a focus on new routes for PU synthesis without requiring either phosgene or isocyanates to conform to special safety, health, and handling precautions and meet the demands of green chemistry and production processes [5].

The reaction between cyclic carbonates and diamines is one of the most promising alternatives to conventional synthesis for designing a PU material without isocyanates [8,9,18,10–17]. The main problem of this route is the limitation for foaming the PU matrix. The main problem with this method is the limitation of foaming the PU matrix. As previously explained, the gas generated by adding a chemical or physical blowing agent and the polymeric matrix generated by the polymerisation reaction are simultaneously produced in conventional PU foams. In contrast, the formation of nonisocyanate PU (NIPU) foams from cyclic carbonates and diamines does not produce gases that would allow material expansion. Thus, an additional physical or chemical blowing agent must be added to the reaction mixture [19]. For instance, Sternberg et al. [20] recently produced NIPU foams using poly(methylhydrosiloxane) as a chemical blowing agent. In 2016, Grignard et al. [19] developed a foaming process by utilising $scCO_2$ as a physical blowing agent. In 2018, Clark et al. [21] achieved self-foaming behaviour, in which the specific reaction between cyclic carbonate and diamine spontaneously liberated CO_2, thereby allowing foam formation.

In this study, we developed NIPU foams via a reaction between trimethylolpropane triscarbonate (tricarbonate) and diamine. Cyclic carbonates are interesting monomers because they are non-toxic [21]. In particular, although safety measures are still necessary during their use, diamines and N-N-dimethylcyclohexylamine (DMCHA) are less harmful to human health than isocyanates [22]. To date, only a few studies related to this synthetic route have been conducted [18,23–28]. In 2015, Cornille et al. [23] developed NIPU foams for the first time by implementing the step-growth polymerisation of two types of cyclic carbonates and diamines using poly(methylhydrogenosiloxane) as a chemical blowing agent, which generates hydrogen gas when it reacts with diamines. The foaming process was performed at high temperatures (80–120 °C). The apparent densities obtained varied in the range of 194–295 kg/m³, and the materials produced exhibited interconnectivity between the cells, measured qualitatively by performing scanning electron microscopy (SEM). In 2016, Cornille et al. [18] improved the last formulation to achieve NIPU foams at room temperature having densities of 270–300 kg/m³, homogeneous microscopic structures with pore sizes of 400–1300 μm, and a large open-cell content. Figovsky et al. [24–26] patented NIPU foams based on epoxy/NIPU hybrid systems. This technique uses epoxy monomers, acrylic monomers, cyclic carbonates and amines as raw materials and hydrofluorocarbons, hydrochlorofluorocarbons, alkylhydrogenosiloxane and also hydrocarbons as physical blowing agents. In 2016, Blattmann et al. [27] developed NIPU foams using a liquid hydrofluorocarbon as the physical blowing agent. The apparent density of the foams was in the range of 142–219 kg/m³, and the cell size was approximately 135 μm. In 2020, Monie et al. [28] explored the formation of self-blown NIPU foams to improve samples previously obtained via reactions between cyclic carbonates, amines, and thiols. In this case, thiols reacted with carbonates to generate CO_2. The density of 166–207 kg/m³ was achieved with cell sizes of 600–980 μm.

In this study, NIPU foams are obtained from tricarbonate and diamine using sodium bicarbonate (SBC) as a chemical blowing agent. SBC is a sustainable chemical that is environmentally compatible and safe for human health. Thus, it has a wide range of applications, such as cooking, cleaning, and hygiene, and can be used as a chemical blowing agent for thermoplastics. Owing to its high availability, non-

flammability, and eco-friendly characteristics and tunability of its decomposition temperatures with respect to the particle size, SBC is a promising alternative to the previously mentioned chemical or physical blowing agents. In the system studied here, the polymerisation reaction between tricarbonate and diamine forms a polymeric matrix in the presence of a catalyst. The thermal decomposition of SBC generates CO_2, which facilitates foam expansion. The effects of SBC having different particle sizes (22, 13, and 3 μm) and contents (5, 10, 15, and 20 wt% with respect to cyclic carbonate) on the density and cellular structure of the resulting NIPU foams are evaluated. Moreover, NIPU formulations having a high SBC content (20 wt% with respect to cyclic carbonate) are optimised by changing the amount of catalyst to obtain foams having reduced densities.

2. Experimental

2.1. Materials

NIPU foams were obtained from two reactants: tricarbonate, which is commercially referenced as SP-3-00-003 (with a functionality of 3, molecular weight of 439.4 g/mol, and purity of 75 wt%) and synthesised by Specific Polymers, and hexamethylene diamine (HMD), which is commercially referenced as H11696 (molecular weight of 116.20 g/mol) and purchased from Sigma-Aldrich. DMCHA, commercially referenced as Polycat® 8 (density of 0.849 g/mL at 25 °C) from Evonik, is a tertiary amine used to promote the reaction between tricarbonate and HMD.

In this study, the chemical blowing agents used were three different grades of SBC from Sigma-Aldrich having different mean particle sizes of 22, 13, and 3 μm.

2.2. Synthesis of the NIPU foams

The formation of the NIPU foams is based on two simultaneous reactions: gelling or polymerisation, which creates a polymeric matrix of PU, and foaming or blowing, which generates the gas needed to expand the material. The synthesis route for the PU foams without isocyanate used in this study is presented in Fig. 1.**a**. The polymerisation reaction is performed by using a cyclic tricarbonate and HMD because cyclic carbonates are amenable to ring opening by suitable nucleophiles, such as amines (aminolysis reactions). The NIPU formulation is adjusted to contain a carbonate group that reactes with an amine group to form a urethane group. This reaction is performed in the presence of DMCHA, which is used as a catalyst for promoting the conversion of the reactants into polyhydroxyurethane products, increasing the degree of cross-linking and, consequently, the viscosity of the mixture. The blowing reaction occurs because of the thermal decomposition of SBC when the reactive mixture is placed in an oven at 150 °C for 6 min to generate CO_2 gas, water, and sodium carbonate (Fig. 1.**b**). The temperature of 150 °C is chosen in this study because the optimum range of the decomposition temperature for SBC is 141–150 °C, as indicated in the literature [29]. The CO_2 produced during the decomposition of SBC facilitates the foam expansion and, consequently, generation of the cellular structure. As the two reactions involved in the generation of NIPU foams occur simultaneously, a balance must be maintained between them to obtain materials having the lowest possible density. For example, when CO_2 gas is formed via SBC decomposition, the reactive mixture must have sufficient viscosity to retain the CO_2 for increased efficiency of the foaming process. However, if the viscosity is excessively high when the gas is released, the expansion ratio should be reduced.

Three series of NIPU foams having different formulations are summarised in Table 1.The samples are prepared as per the procedure depicted in Fig. 1.**b**. First, tricarbonate is mixed with the respective amounts of SBC in a mould (diameter of 2 cm and height of 3.5 cm) at
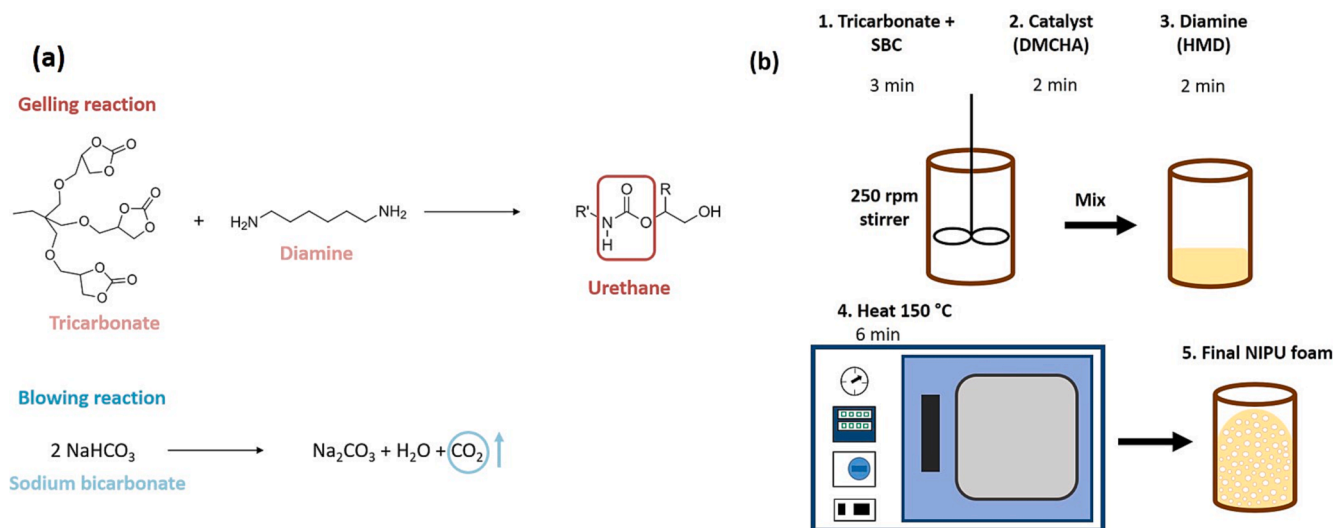
Fig. 1. (a) New route to synthesize NIPU foams from cyclic carbonates and diamines using sodium bicarbonate as chemical blowing agent and (b) lab route to produce the samples.

Table 1

Formulation of NIPU foams with different SBC types (22 μm, 13 μm and 3 μm) and several SBC contents.

NIPU foams with different SBC types	SBC (g)	Tricarbonate (g)	HMD (g)	Catalyst (μl)
5 wt% SBC	0.05	1	0.4	5.9
10 wt% SBC	0.10	1	0.4	5.9
15 wt% SBC	0.15	1	0.4	5.9
20 wt% SBC	0.20	1	0.4	5.9

250 rpm for 3 min using an overhead stirrer (EUROESTAR 60 control from IKA) with an R 1002 screw-type stirrer. Subsequently, the 0.5 wt% DMCHA catalyst (respect to the mass of tricarbonate) is mixed into the blend at 250 rpm for 2 min. The corresponding amount of HMD is stirred with the previous mixture at 250 rpm for 2 min to initiatethe polymerization reaction. Finally, all the mixtures are heated in an oven (E-42, Heraeus) at 150 °C for 6 min to promote SBC decomposition, thereby generating gas and expanding the material. The mixture is then cooled to room temperature (between 20 and 25 °C). Next, the formulation of the NIPU foams with high SBC contents is optimised by varying the amount of catalyst, as shown in Table 2.

2.3. SBC characterisation

The size of the SBC particles used in this study was measured via laser diffraction using an LS 13 320 analyser (Beckman Coulter). The chemical composition was determined by performing Fourier transform infrared (FTIR) spectroscopy using a Bruker Tensor 27 spectrometer in the attenuated total reflectance (ATR) mode. SBC decomposition was studied by conducting thermogravimetric analysis (TGA) from 50 to 1000 °C at a heating rate of 20 °C/min under an inert atmosphere (N_2) using a Mettler Toledo TGA/SDTA 851.

Table 2

Formulation of NIPU foams optimized with different SBC types (22 μm, 13 μm and 3 μm).

NIPU foams with different SBC types	SBC (g)	Tricarbonate (g)	HMD (g)	Catalyst (μl)
20 wt% SBC_0.5 wt% CAT	0.20	1	0.4	**5.9**
20 wt% SBC_1.5 wt% CAT	0.20	1	0.4	**17.7**
20 wt% SBC_2 wt% CAT	0.20	1	0.4	**23.6**

2.4. Foam characterisation

2.4.1. Density

The density of the foams (ρ_f) was determined by employing the water-displacement method based on Archimedes' principle (**Eq. (1)**) using a density determination kit for an AT261 Mettler-Toledo balance.

$$\rho_f = \frac{W_{f,air}}{W_{f,air} - W_{f,water}}\rho_{water} \tag{1}$$

where, $w_{f,\,air}$ is the weight of the foam in air, $w_{f,water}$ represents the weight of the foam in water and ρ_{water} denotes the density of water.

2.4.2. Open cell content

To measure the percentage of open cells in the foams, namely, the open-cell content (OC%), a gas pycnometer (AccuPyc II 1340, Micromeritics) was used as per the procedure described in the ASTM D6226-10 standard [30]. The following equation provides the value of this parameter:

$$OC(\%) = \frac{Interconected\ cells\ volume}{Total\ gas\ volume} = \frac{V_{sample} - V_{pycnometer} - V_{exposedcells}}{V_{sample}(1 - \rho_r)} \tag{2}$$

where, v_{sample} is the volume of the foam calculated as the ratio of the weight of the foam to the density measured by using Archimedes' principle, $v_{pycnometer}$ is the volume determined by employing the pycnometer, $v_{exposed}$ cells is the volume occupied by the cells on the surface of the samples used for these measurements and ρ_r is the relative density calculated as the ratio of the density of the foam (ρ_f) to the density of the corresponding solid polymer (ρ_s).

Cylindrical samples having radius r and height h were used for the measurements. $v_{exposed}$ cells, which accounts for the volume of the cells on the surface of the samples, was calculated by applying the following equation as per the ASTM D6226-10 standard:

$$V_{exposed} = \frac{A\phi_{2D}}{1.14} \tag{3}$$

In which φ_{2D} is the average two-dimensional (2D) cell size obtained from the SEM micrographs, as A is the geometric surface area of the specimen and calculated as follows:

$$A = 2\pi r^2 + 2\pi rh \tag{4}$$

where r is the radius of the sample and is considered to be the radius of

the mould, and *h* is the height of the cylinder.

The thermal decomposition of SBC produces sodium carbonate particles that remain in the PU matrix as fillers, modifying the density of the solid polymer. Therefore, the rule of mixtures for a compound of solid PU and sodium carbonate must be applied to obtain the ρ_s for each foam having different SBC contents, assuming that the amount of sodium carbonate in the blend is 64% of the SBC mass introduced into the initial formulation (Fig. 2.**a**).

2.4.3. Scanning electron microscopy (SEM)

SEM was used to investigate the surface morphology of the NIPU foams. The cellular structures of the samples were analysed using a FlexSEM 1000 VP-SEM instrument (Hitachi). For correct visualisation, the samples were fractured in liquid nitrogen to preserve their original cellular structures. The sample surfaces were then coated with gold using a sputter coater (model SDC 005, Balzers Union, Balzers, Liechtenstein) and finally visualised in the growth plane. Several parameters were measured to obtain a complete analysis of the cellular structure. A tool based on the ImageJ/FIJI software[31] was used to quantify these structural parameters. The average three-dimensional (3D) cell size ($\phi3D$) was determined by multiplying the 2D values measured in the SEM image by the correction factor of 1.273 [31]. Moreover, the standard deviation (SD) coefficient of the cell size distribution SD/ ϕ (normalised standard deviation coefficient) calculated as an indicator of the homogeneity of the cellular structure, and anisotropy ratio were determined for comparison between the materials. In addition, cell density (N_v) which is the number of cells per unit volume of foam (cells/cm^3) was determined according to **Eq. (5)**, taking into account the density of both the solid polymer (ρ_s), foam samples (ρ_f) and $\phi3D$ [31].

$$N_v = \frac{6(1 - \frac{\rho_f}{\rho_s})}{\pi(\phi_{3D})^3} \qquad (5)$$

The cell nucleation density ($N0$) was determined using **Eq. (6)**. This parameter measures the number of cells per cubic centimetre of solid material or unfoamed material (nuclei/cm^3) assuming that degeneration does not occur during the processing, this means that every nucleation point in the solid becomes a cell in the foamed material [31].

$$N_0 = \frac{N_v}{\rho_{f/\rho_s}} \qquad (6)$$

2.4.4. FTIR spectroscopy

FTIR analysis of the final foams was performed 1 day after foam production to verify the completely consumption of the reactants to form the products (urethane groups). The comparison of the spectra revealed the bands associated with tricarbonate (carbonyl stretching band at 1790 cm^{-1}) and HMD (NH stretching bands between 3500 and 3000 cm^{-1}) and the carbonyl band associated with the urethane group formed at 1695 cm^{-1}[18]. The FTIR spectra were recorded on a Bruker Tensor 27 spectrometer by employing the ATR mode.

3. Results and discussion

3.1. Characterization of the SBC

A bimodal particle size distribution is detected for all the materials (Fig. 2). The mean particle sizes obtained for each type of SBC and the key parameters of the particle size distributions are listed in Table 3. As expected, clear differences are present among the three SBC grades.

The mass loss of the SBC particles (Fig. 3) is ascribed to the decomposition of SBC into CO_2, water, and sodium carbonate (Fig. 1.**a**). A comparison of all the SBC reveals three different decomposition rates; the decomposition rate increases as the particle size decreases (Fig. 3.**a**). This behaviour is important for the production of NIPU foams because
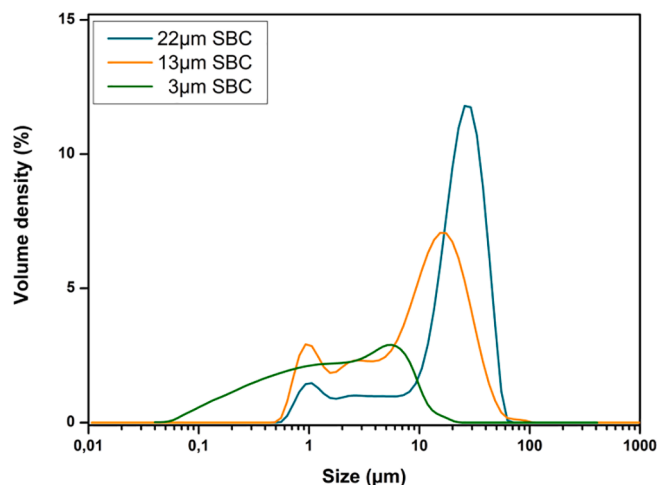

Fig. 2. Particle Size distribution of the three SBC.

gas formation occurs earlier in the foams produced using smaller particles. Moreover, the residue obtained is 64% for all the SBC, corresponding to the sodium carbonate formed in the SBC decomposition that remains as a filler in the PU matrix. Fig. 3.**b** shows the first derivative of the thermograms, in which the minimum value is considered to be the mean decomposition temperature. These mean decomposition temperatures are 145.7, 137.9, and 133.8 °C for the SBC having the size of 22, 13, and 3 μm, respectively; thus, these temperatures are below 150 °C (temperature used for foaming) for all the particles. Moreover, a significant temperature difference of 12 ̊C exists between the smaller and larger particles.

3.2. NIPU foams produced with different types of SBC

Fig. 4 shows the FTIR spectra of the reactants and foam. The largest amount of SBC decomposes at higher temperatures. Polymerisation is completed under the experimental conditions because the bands associated with tricarbonate and HMD do not appear in the spectrum of the NIPU foam. Similar results are observed for other NIPU foams. Moreover, the bands associated with the SBC particles (Fig. 4.**d**) do not appear in the spectrum of the final foams (Fig. 4.**c**), demonstrating the decomposition of all SBC during foam production.

Density is one of the most important parameters because it determines the performance, cost, and in many cases, final applications of foams. The measured density values are shown in Fig. 5. The density is expected to decrease as the amount of SBC increases, generating more CO_2 gas during particle decomposition. However, this trend is not observed in any of the NIPU foam series studied. This unexpected behaviour can be ascribed to the different balances of the two simultaneous processes involved in the synthesis of the NIPU foams (Fig. 1.**a**).

Moreover, any change in the particle size or catalyst content may affect the kinetics. The SBC having the particle size of 22 μm exhibits a behaviour closer to the expected trend. For this system, increasing the amount of the blowing agent reduces the density until it reaches an almost constant value of approximately 15 wt% content. This behaviour indicates that the viscosity of the polymeric system is sufficiently high to retain large amounts of CO_2 when SBC is released. This may be related to the delayed gas release of this specific SBC (Fig. 3). Meanwhile, the SBC having a particle size of 3 μm releases gas earlier, decreasing the viscosity of the gas and allowing a higher expansion at low SBC concentrations. However, this lower viscosity decreases the stability of the system, and larger amounts of SBC promote higher-density foams owing to the gas that cannot be retained and/or degeneration of the cellular structure. Note that this is a qualitative explanation of the behaviour of these complex systems. The complexity of the samples in terms of the foaming temperature and sample size limits the in situ measurements in

Table 3
Main parameters of the size distribution of the SBCs used in this study.

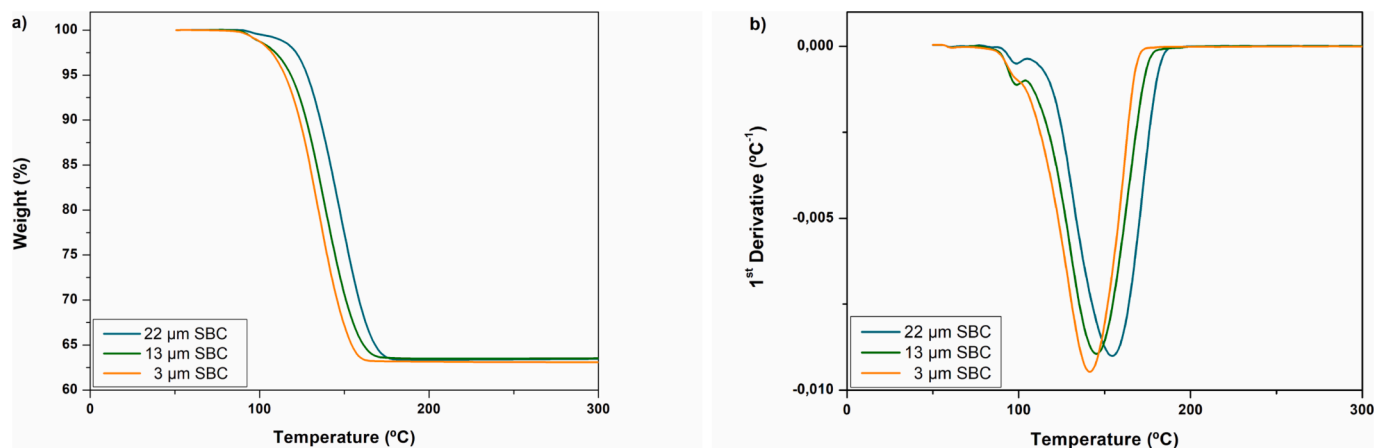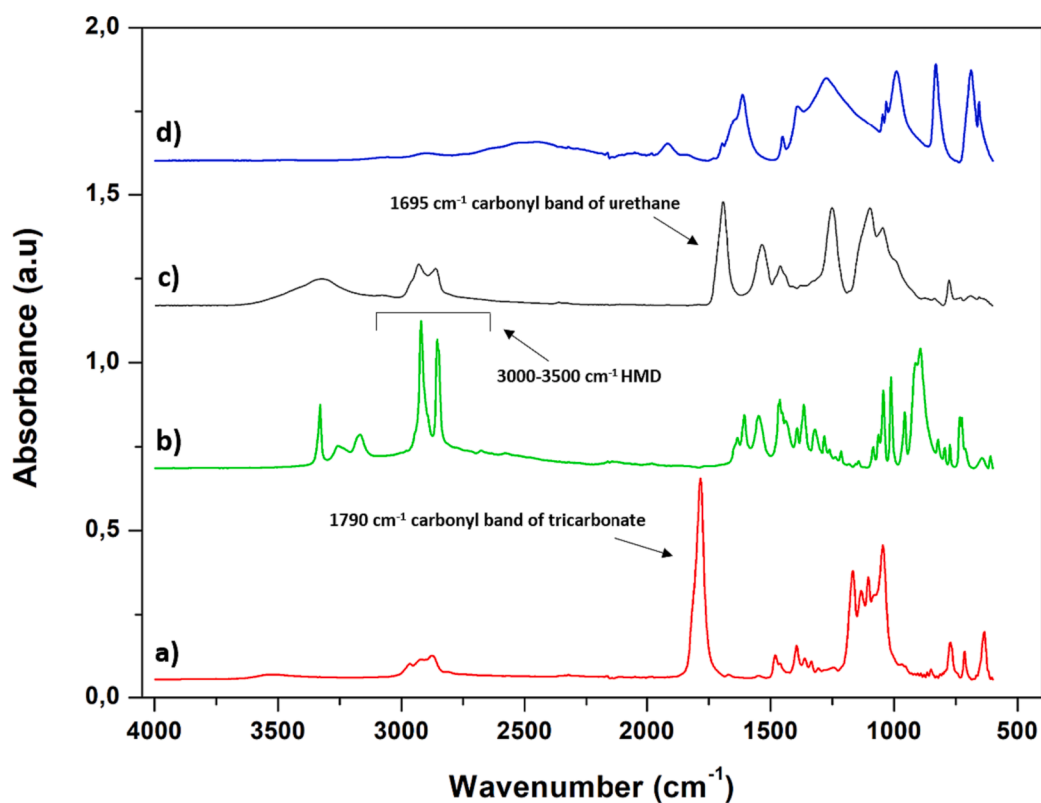| SBC particles	D10 (μm)	D50 (μm)	D90 (μm)	Mean particle size (μm)	Mean size of the first peak in the bimodal distribution (μm)	Mean size of the second peak in the bimodal distribution (μm)
22 μm	2.7	22.6	39.6	22	9.2	24.3
13 μm	1.2	10.8	27.8	13	1.1	18.7
3 μm	0.2	1.8	7.8	3	1.3	7.1

Fig. 3. (a) TGA thermograms and (b) first derivative of the decomposition curve for the different SBC particles under study.

Fig. 4. FTIR spectra of (a) tricarbonate, (b) HMD, (c) 20 wt%. 22 μm SBC foam used as an example, and (d) 22 μm SBC.

quantifying the foaming mechanisms and reaction kinetics in detail. For the type and amount of catalyst employed in the formulations of these foams, the SBC having a particle size of 13 μm achieves the optimum values, suggesting the promoted formation of foams having lower densities. Therefore, for this specific system, a good balance exists between the polymerisation and blowing reactions for SBC contents of up to 15 wt%. A higher SBC content promotes a distinctive increase in density.

The SEM micrographs of the samples are shown in Fig. 6. The materials have a significant number of open cells and slight anisotropy in the growth direction. In addition, in several cases, such as SBC having a particle size of 3 μm and high SBC content, highly degenerated structures are observed. The materials having low densities for each series
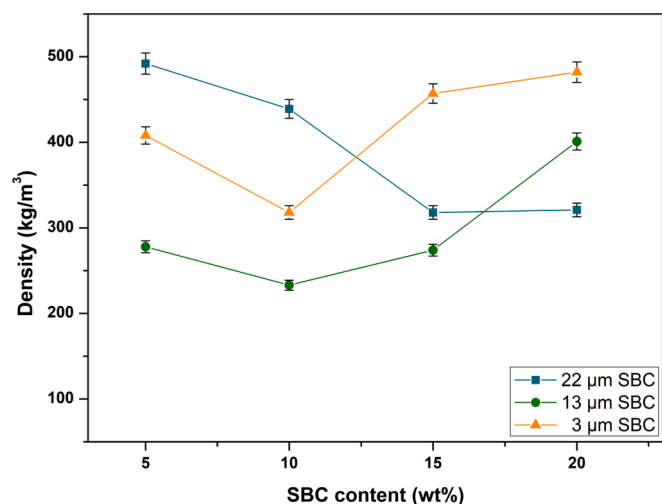
Fig. 5. Density of the NIPU foams obtained with different types of SBC as a function of the SBC content.

show more homogeneous structures. Moreover, the materials produced with SBC having larger particle sizes exhibit the most homogeneous structures.

The other parameters of the cellular structure are listed in Table 4. All the foams have a significant number of open cells, with open-cell

content of 60%–100%. In particular, a reduction in the particle size increases the open-cell content. The cell size increases as the foam density decreases. Smaller cell sizes are obtained for the materials produced with the SBC particle size of 3 μm.

The values of the NSD are in the range of 0.4–0.9 and not dependent on the density. The SBC having the particle size of 13 μm results in the most heterogeneous materials. The foams exhibit anisotropy ratios greater than one, indicating a slight degree of orientation along the growth direction. The materials produced using SBC having the particle size of 3 μm have the largest anisotropy. Finally, the cell density and nucleation density increase with the density. As such, the materials with SBC having the particle size of 3 μm achieve the largest value for these parameters.

The theoretical density of the NIPU foams is calculated by applying the following equation:

$$\rho_f = \frac{\left(1 - \frac{0.6X_{SBC}^P}{\rho_{SC}}\right)\rho_{PU} + 0.6X_{SBC}^P}{\left\{X_{SBC}^P \varphi \left[\left(1 - \frac{X_{SBC}^P}{\rho_{SBC}}\right)\rho_{PU} + X_{SBC}^P\right]\right\} + 1} \tag{7}$$

where ρ_{PU} is the density of the solid PU matrix (1190 kg/m³), ρ_{SBC} is the density of SBC (2200 kg/m³), and ρ_{SC} is the density of sodium carbonate (SBC residue, 2710 kg/m³). The gas yield of the SBC was assumed to be $\varphi = 80$ cm³/g = 0.08 m³/kg. This equation is formulated by assuming ideal conditions, in which all the CO_2 generated is used in the foaming process and no gas escapes from the system. Fig. 7 shows the behaviour obtained using **Eq. (7)** as the number of SBC particles increases. Note
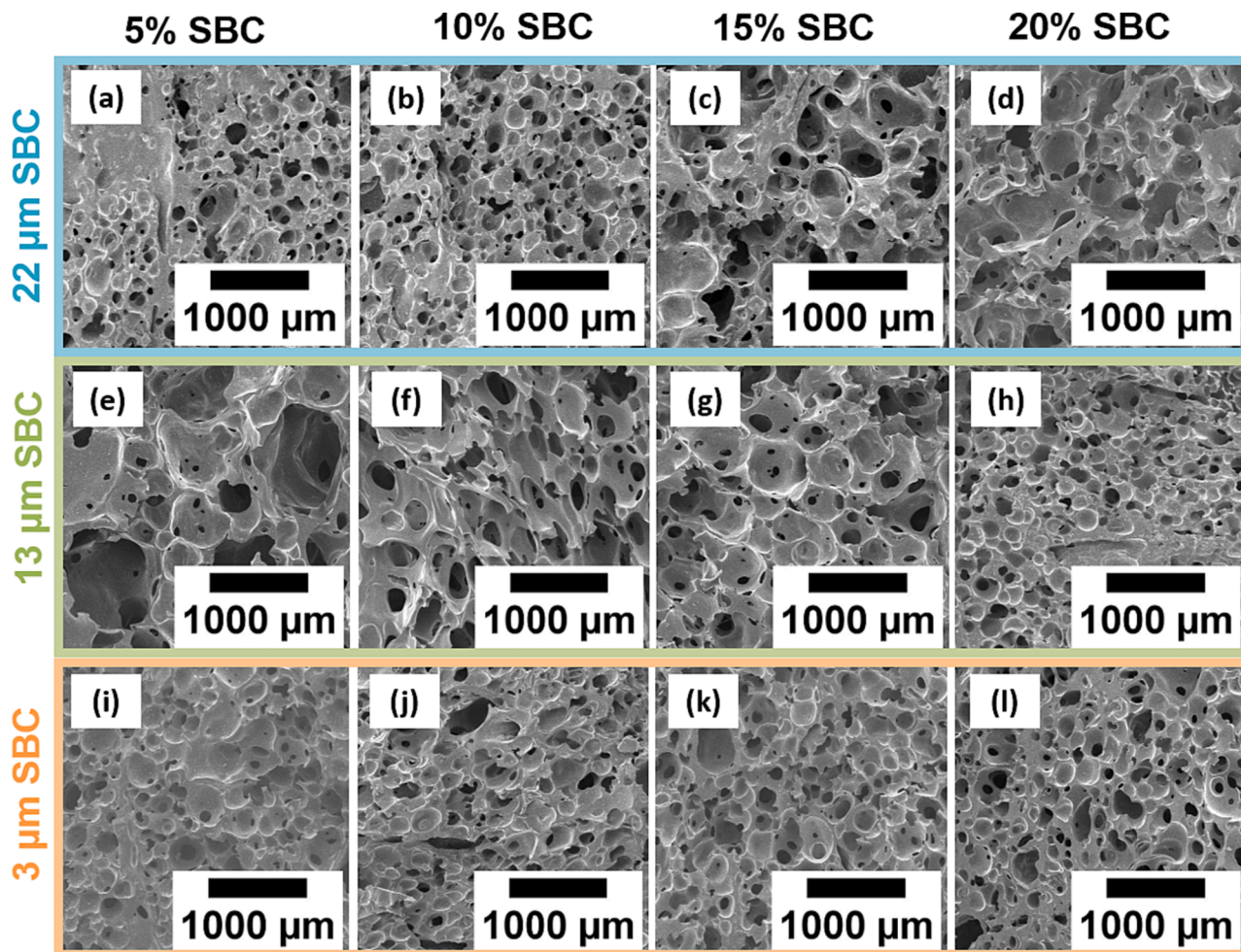

Fig. 6. Representative SEM images of the cellular structure of the NIPU foams: (a) 5% SBC 22 μm, (b) 10% SBC 22 μm, (c) 15% SBC 22 μm, (d) 20% SBC 22 μm, (e) 5% SBC 13 μm, (f) 10% SBC 13 μm, (g) 15% SBC 13 μm, (h) 20% SBC 13 μm, (i) 5% SBC 3 μm, (j) 10% SBC 3 μm, (k) 15% SBC 3 μm, (l) 20% SBC 3 μm.

Table 4
Cellular structure characterization of the NIPU foams.

Sample	Density (kg/m³)	OC (%)	Cell Size (μm)	NSD	A	N_0 (nuclei/cm³)	N_v (cells/cm³)
5% SBC 22 μm	492 ± 12	60.0 ± 3	168 ± 16.8	0.52	1.07 ± 0.11	5.87×10^5	2.40×10^5
10% SBC 22 μm	439 ± 11	66.2 ± 3	173 ± 17.3	0.49	1.13 ± 0.11	6.53×10^5	2.35×10^5
15% SBC 22 μm	318 ± 8	82.6 ± 4	262 ± 26.2	0.62	1.11 ± 0.11	3.06×10^5	7.89×10^4
20% SBC 22 μm	321 ± 8	78.9 ± 4	348 ± 34.8	0.47	1.10 ± 0.11	1.30×10^5	3.36×10^4
5% SBC 13 μm	278 ± 7	76.7 ± 4	376 ± 37.6	0.83	1.14 ± 0.11	1.20×10^5	2.77×10^4
10% SBC 13 μm	233 ± 6	83.9 ± 4	322 ± 32.2	0.84	1.21 ± 0.12	2.41×10^5	4.61×10^4
15% SBC 13 μm	274 ± 7	72.2 ± 4	342 ± 34.2	0.56	1.03 ± 0.10	1.67×10^5	3.72×10^4
20% SBC 13 μm	401 ± 10	86.8 ± 4	162 ± 16.2	0.57	1.17 ± 0.12	9.40×10^5	3.02×10^5
5% SBC 3 μm	408 ± 10	95.3 ± 5	227 ± 22.7	0.64	1.09 ± 0.11	3.19×10^5	1.08×10^5
10% SBC 3 μm	318 ± 8	77.7 ± 4	171 ± 17.1	0.44	1.19 ± 0.12	1.08×10^6	2.82×10^5
15% SBC 3 μm	457 ± 11	96.0 ± 5	186 ± 18.6	0.50	1.25 ± 0.13	5.06×10^5	1.88×10^5
20% SBC 3 μm	482 ± 12	84.1 ± 4	174 ± 17.4	0.50	1.34 ± 0.13	5.76×10^5	2.23×10^5

Table 5
Amount of SBC used in this work expressed in grams, the corresponding mass fraction of SBC (X_{SBC}^P) and theoretical density of the resulting NIPU foams.

SBC mass introduced in the foam (g)	Mass fraction of SBC (X_{SBC}^P)	Theoretical density of foams with different contents of SBC (ρ_f) (kg/m³)
0.05	0.0345	278
0.10	0.0667	162
0.15	0.0968	117
0.20	0.1250	92

SBC (Table 5).

Different trends are observed for the theoretical (Table 5) and experimental densities (Fig. 5); the experimental values are well above the theoretical values. As previously discussed, an increase in the SBC content is not always related to a density reduction. Several reasons exist for the differences between the expected and actual densities. On one hand, **Eq. (7)** assumes that all the gases released by the SBC are used to reduce the density, which is clearly incorrect because gas diffuses out of the system, especially in the early stages of foaming. On the other hand, this model does not consider the cell opening and the escape of gases from the formed cells when the cells are connected. As such, we need an optimised foaming process to achieve a high viscosity sufficient for the early stages of foaming to reduce gas escape, cell opening, and coalescence phenomena, thereby reaching values similar to those predicted by applying **Eq. (7)**.

3.3. Optimisation of the formulation of the NIPU foams

Formulation modification aims to determine the minimum density for each system. An increase in the catalyst content promotes the degree of polymerisation to retain higher amounts of gas generated during SBC decomposition. The densities of the foams are shown in Fig. 8 and Table 6. The cellular structure parameters are listed in Table 6, and the SEM micrographs are displayed in Fig. 9. As shown in Fig. 8, in the foams having 0.5 wt% catalyst, the polymeric matrix cannot retain the generated gas, and the density is excessively high for the three blowing agents used. In addition, with 2 wt% catalyst, the degree of polymerisation is excessive, inhibiting the expansion of the matrix by the gas. In both cases, the densities are extremely high. In contrast, the lowest densities are achieved with 1.5 wt% of catalyst. This trend is observed for all three SBC foam series. Although the theoretical values are not achieved, the values obtained improve compared with the previous results. In particular, the smallest value is achieved with 3-μm SBC; it is 142 kg/m³, which is extremely low compared with the value obtained

that this equation is formulated by considering that 64% of the SBC used in the formulation remains in the foam as sodium carbonate, that is, as a filler, which increases the density of the polymeric matrix.

Table 5 shows the expected density values obtained from **Eq. (7)**.

An adequate mass fraction of the SBC introduced into the foam must be considered to determine the expected theoretical values. Therefore, these fractions are recalculated with respect to the total mass of the blend, that is, the masses of tricarbonate (1 g) and HMD (0.4 g) added to
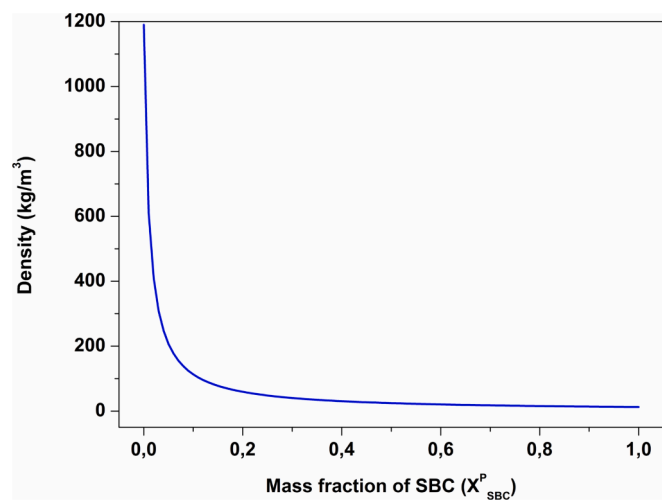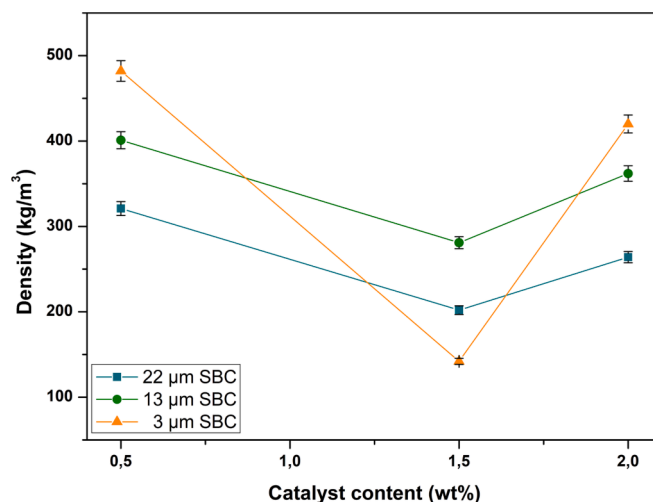

Fig. 7. Evolution of theoretical density when the mass fraction of SBC (X_{SBC}^P) is changed.

Fig. 8. Density of the optimized NIPU foams changing the amount of catalyst.

Table 6

Cellular structure characterization of optimized NIPU foams.

| Sample	Density (kg/m³)	OC (%)	Cell Size (µm)	NSD	A	N_0 (nuclei/ cm³)	N_v (cells/ cm³)
22 µm SBC_0.5 % CAT	321 ± 8	78.86 ± 4	348 ± 35	0.47	1.10 ± 0.11	1.30×10^5	3.36×10^4
22 µm SBC_1.5% CAT	**202 ± 5**	**90.53 ± 5**	**362 ± 36**	**0.59**	**1.10 ± 0.11**	**2.09×10^5**	**3.38×10^4**
22 µm SBC_2% CAT	264 ± 7	80.84 ± 4	375 ± 38	0.54	1.23 ± 0.12	1.35×10^5	2.86×10^4
13 µm SBC_0.5 % CAT	401 ± 10	86.81 ± 4	162 ± 16	0.57	1.17 ± 0.12	9.40×10^5	3.02×10^5
13 µm SBC_1.5% CAT	**281 ± 7**	**88.56 ± 4**	**461 ± 46**	**0.75**	**1.01 ± 0.10**	**6.70×10^4**	**1.51×10^4**
13 µm SBC_2% CAT	362 ± 9	–	–	–	–	–	–
3 µm SBC_0.5 % CAT	482 ± 12	84.13 ± 4	174 ± 17	0.50	1.34 ± 0.13	5.76×10^5	2.23×10^5
3 µm SBC_1.5% CAT	**142 ± 4**	**89.97 ± 4**	**329 ± 33**	**0.58**	**1.05 ± 0.11**	**4.17×10^5**	**4.75×10^4**
3 µm SBC_2% CAT	420 ± 11	–	–	–	–	–	–
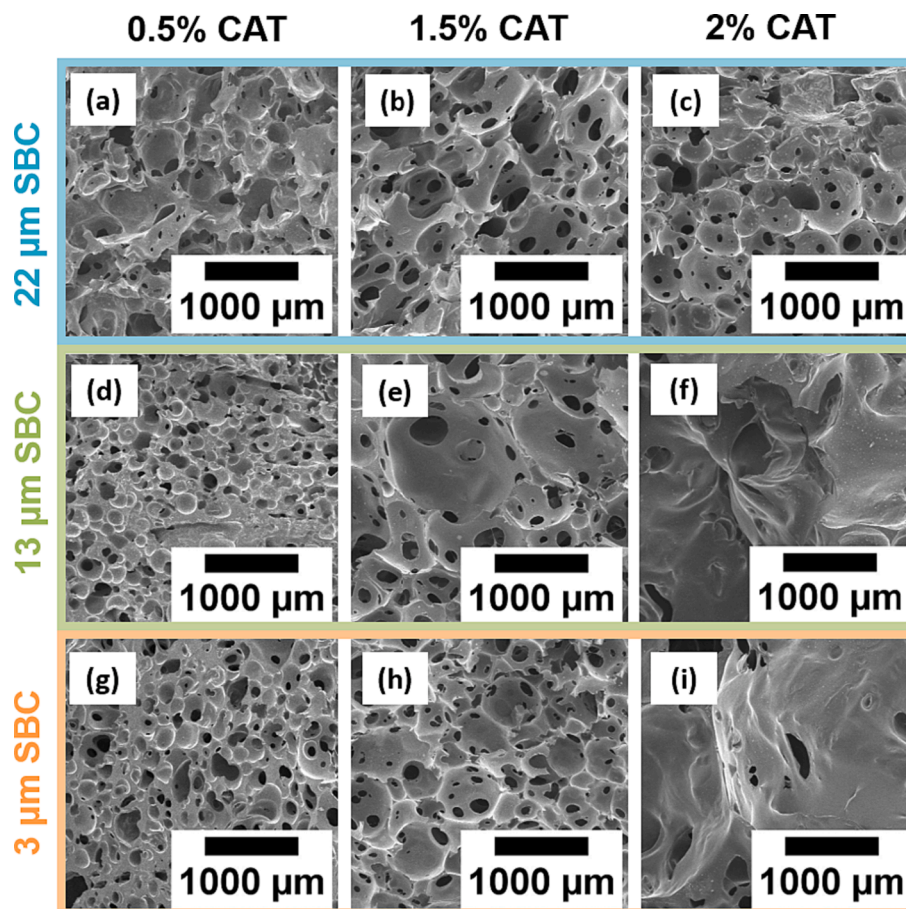
Fig. 9. SEM micrographs of the optimized NIPU foams with 20 wt% SBC: (a) 22 µm SBC_0.5 % CAT, (b) 22 µm SBC_1.5 % CAT, (c) 22 µm SBC_2 % CAT, (d) 13 µm SBC_0.5 % CAT, (e) 13 µm SBC_1.5 % CAT, (f) 13 µm SBC_2 % CAT, (g) 3 µm SBC_0.5 % CAT, (h) 3 µm SBC_1.5 % CAT, (i) 3 µm SBC_2 % CAT.

with 0.5 wt% catalyst (482 kg/m³).

The values of the cell size for the optimum foams are in the range of 330–460 µm. The material produced with the smallest particle is obtained using the minimum cell size of 330 µm. Most of the materials show an open-cell content higher than 80% and an anisotropic cellular structure, with slightly elongated the cells in the growth direction. The cell nucleation densities are in the order of 10^4 nuclei/cm³, which is the value for the foam having the lowest density of 4.75×10^4 nuclei/cm³. The materials produced with a higher catalyst content and SBC having particle sizes of 13 and 3 µm cannot be quantitatively characterised using SEM because of their high heterogeneity. For these materials, the high viscosity of the polymer does not facilitate a proper foaming of the system. Therefore, we can summarise that proper optimisation of the catalyst content can produce NIPU foams having lower densities (i.e. the

minimum density of 142 kg/m³ with a porosity of 89%) and a homogenous open-cell cellular structure with the average cell size of 329 µm. Among all the catalyst contents used, the optimum foams are obtained with 1.5 wt% catalyst owing to their lower differences from the theoretical values (92 kg/m³ for 20 wt% SBC). In particular, the lowest density reached differs from the theoretical value by a factor of 1.5, because of the strong capacity of the theoretical model to estimate density as an expected difference. In addition, our lowest density is similar to that reported by Blattmann et al. [27]. The SBC particles providing the optimum results have a smaller size (3 µm) and a lower decomposition temperature.

4. Conclusions

In this study, a new synthesis route for NIPU foams using SBC as a chemical blowing agent was developed for the first time. The use of this chemical blowing agent is a sustainable approach for developing NIPU foams.

SEM, laser diffraction, FTIR spectroscopy, and TGA were used to characterise the SBC particles having sizes of 22, 13, and 3 μm. Three series of NIPU foams were synthesised for each type of SBC having different SBC contents (5, 10, 15, and 20 wt%). The effects of the different types and contents of SBC on the density and cellular structure of the resulting NIPU foams were evaluated. The density decreased as the SBC content increased because more CO_2 was produced during SBC decomposition. However, a reduction in this value was not observed for all SBC types as the amount of the chemical blowing agent was increased. The expected densities depended on the balance between two simultaneous reactions: the polymerisation reaction between tricarbonate and diamine, which formed the polymeric matrix, and the decomposition of the SBC particles, which generated CO_2 to expand the polymer. Therefore, the initial formulations tested did not have a proper balance between the polymerisation and foaming reactions because each type of SBC decomposed at different times (decomposition was accelerated for smaller SBC sizes). For the material that underwent rapid SBC decomposition, the degree of polymerisation was extremely low; thus, the PU matrix was unable to entrap all the formed CO_2. This particularly occurred for the NIPU foams having 3-μm SBC because of the highest decomposition rate. Consequently, these foams exhibited the highest densities.

The foam formulation was optimised by increasing the amount of catalyst to obtain materials having the desired densities. The increase in the catalyst content promoted the polymerisation reaction for retaining the gas generated during the SBC decomposition. This formulation was optimised for foams having high SBC contents because these materials have considerable potential for density reduction, considering the high amount of SBC used. Among the three NIPU foams the foam having the lowest density was obtained with 1.5 wt% catalyst. The lowest density of 142 kg/m^3 was achieved for the NIPU foam having the SBC of 3 μm, corresponding to a porosity of 89%. This material exhibited a homogenous open-cell cellular structure with an average cell size of 329 μm. The route proposed in this study could be further optimised by further reducing the SBC particle size and fine-tuning the polymerisation kinetics of the polymeric matrix. Further, the kinetics of both reactions should be properly adjusted to obtain low-density homogeneous NIPU foams.

CRediT authorship contribution statement

Clara Amezúa-Arranz: Conceptualization, Methodology, Investigation, Formal analysis, Writing – original draft. **Mercedes Santiago-Calvo:** Conceptualization, Investigation, Supervision, Writing - review & editing. **Miguel-Ángel Rodríguez-Pérez:** Conceptualization, Supervision, Funding acquisition, Writing - review & editing.

Declaration of Competing Interest

The authors declare that they have no known competing financial interests or personal relationships that could have appeared to influence the work reported in this paper.

Data availability

No data was used for the research described in the article.

Acknowledgements

References

[1] O. Bayer, Das Di-Isocyanat-Polyadditionsverfahren (Polyurethane), Angew. Chem. 59 (9) (1947) 257–272, https://doi.org/10.1002/ange.19470590901.

[2] The Future of Polymer Foams to 2026., (n.d.). https://www.smithers.com/servi ces/market-reports/materials/the-future-of-polymer-foams-to-2019.

[3] M. Santiago-Calvo, V. Blasco, C. Ruiz, R. París, F. Villafañe, M.Á. Rodríguez-Pérez, Improvement of thermal and mechanical properties by control of formulations in rigid polyurethane foams from polyols functionalized with graphene oxide, J. Appl. Polym. Sci. 136 (2019) 1–10, https://doi.org/10.1002/app.47474.

[4] E. Kollia, K. Andreopoulou, V. Kostopoulos, Development and mechanical characterization of a non-isocyanate rigid polyurethane foam, Res. Develop. Mater. Sci. 10 (3) (2020), https://doi.org/10.31031/rdms.2019.10.000738.

[5] N. Gama, A. Ferreira, A. Barros-Timmons, Polyurethane foams: Past, present, and future, Materials 11 (10) (2018) 1841, https://doi.org/10.3390/ma11101841.

[6] G. Rokicki, P.G. Parzuchowski, M. Mazurek, Non-isocyanate polyurethanes: synthesis, properties, and applications, Polym. Adv. Technol. 26 (2015) 707–761,, https://doi.org/10.1002/pat.3522.

[7] D.C. Allport, D.S. Gilbert, S.M. Outterside, MDI and TDI: Safety, Health and the Environment: A Source Book and Practical Guide (2003), https://doi.org/10.1002/ 0470865687.

[8] M. Bähr, R. Mülhaupt, Linseed and soybean oil-based polyurethanes prepared via the non-isocyanate route and catalytic carbon dioxide conversion, Green Chem. 14 (2012) 483–489, https://doi.org/10.1039/c2gc16230j.

[9] M. Bähr, A. Bitto, R. Mülhaupt, Cyclic limonene dicarbonate as a new monomer for non-isocyanate oligo- and polyurethanes (NIPU) based upon terpenes, Green Chem. 14 (2012) 1447–1454, https://doi.org/10.1039/c2gc35099h.

[10] M. Fleischer, H. Blattmann, R. Mülhaupt, Glycerol-, pentaerythritol- and trimethylolpropane-based polyurethanes and their cellulose carbonate composites prepared via the non-isocyanate route with catalytic carbon dioxide fixation, Green Chem. 15 (2013) 934–942, https://doi.org/10.1039/c3gc00078h.

[11] X. Sheng, G. Ren, Y. Qin, X. Chen, X. Wang, F. Wang, Quantitative synthesis of bis (cyclic carbonate)s by iron catalyst for non-isocyanate polyurethane synthesis, Green Chem. 17 (2015) 373–379, https://doi.org/10.1039/c4gc01294a.

[12] Q. Chen, K. Gao, C. Peng, H. Xie, Z.K. Zhao, M. Bao, Preparation of lignin/glycerol-based bis(cyclic carbonate) for the synthesis of polyurethanes, Green Chem. 17 (2015) 4546–4551, https://doi.org/10.1039/c5gc01340b.

[13] H. Blattmann, R. Mülhaupt, Multifunctional β-amino alcohols as bio-based amine curing agents for the isocyanate- and phosgene-free synthesis of 100% bio-based polyhydroxyurethane thermosets, Green Chem. 18 (2016) 2406–2415, https://doi. org/10.1039/c5gc02563j.

[14] S.E. Dechent, A.W. Kleij, G.A. Luinstra, Fully bio-derived CO2 polymers for non-isocyanate based polyurethane synthesis, Green Chem. 22 (2020) 969–978, https://doi.org/10.1039/c9gc03488a.

[15] C. Zhang, H. Wang, Q. Zhou, Waterborne isocyanate-free polyurethane epoxy hybrid coatings synthesized from sustainable fatty acid diamine, Green Chem. 22 (2020) 1329–1337, https://doi.org/10.1039/c9gc03335a.

[16] H. Chen, P. Chauhan, N. Yan, "Barking" up the right tree: biorefinery from waste stream to cyclic carbonate with immobilization of CO2for non-isocyanate polyurethanes, Green Chem. 22 (2020) 6874–6888, https://doi.org/10.1039/ d0gc02285c.

[17] X. Yang, S. Wang, X. Liu, Z. Huang, X. Huang, X. Xu, H. Liu, D. Wang, S. Shang, Preparation of non-isocyanate polyurethanes from epoxy soybean oil: Dual dynamic networks to realize self-healing and reprocessing under mild conditions, Green Chem. 23 (2021) 6349–6355, https://doi.org/10.1039/d1gc01936h.

[18] A. Cornille, C. Guillet, S. Benyahya, C. Negrell, B. Boutevin, S. Caillol, Room temperature flexible isocyanate-free polyurethane foams, Eur. Polym. J. 84 (2016) 873–888, https://doi.org/10.1016/j.eurpolymj.2016.05.032.

[19] B. Grignard, J. Thomassin, S. Gennen, L. Poussard, L. Bonnaud, J.M. Raquez, P. Dubois, M.P. Tran, C.B. Park, C. Jerome, C. Detrembleur, CO2-blown microcellular non-isocyanate polyurethane (NIPU) foams: From bio- and CO2-sourced monomers to potentially thermal insulating materials, Green Chem. 18 (2016) 2206–2215, https://doi.org/10.1039/c5gc02723c.

[20] J. Sternberg, S. Pilla, Materials for the biorefinery: High bio-content, shape memory Kraft lignin-derived non-isocyanate polyurethane foams using a non-toxic protocol, Green Chem. 22 (2020) 6922–6935, https://doi.org/10.1039/ d0gc01659d.

[21] J.H. Clark, T.J. Farmer, I.D.V. Ingram, Y. Lie, M. North, Renewable Self-Blowing Non-Isocyanate Polyurethane Foams from Lysine and Sorbitol, Eur. J. Org. Chem. 2018 (2018) 4265–4271, https://doi.org/10.1002/ejoc.201800665.

[22] P.S. Choong, K.W.E. Tam, N.X. Chong, A.M. Seayad, J. Seayad, S. Jana, Biobased, Biodegradable, and Water-Soluble Amine-Functionalized Non-Isocyanate Polyurethanes for Potential Home Care Application, ACS Appl. Polym. Mater. 5 (7) (2023) 5503–5513, https://doi.org/10.1021/acsapm.3c00827.

[23] A. Cornille, S. Dworakowska, D. Bogdal, B. Boutevin, S. Caillol, A new way of creating cellular polyurethane materials: NIPU foams, Eur. Polym. J. 66 (2015) 129–138, https://doi.org/10.1016/j.eurpolymj.2015.01.034.

[24] O. Figovsky, R. Potashnikov, A. Leykin, L. Shapovalov, S. Sivokon, Method for Forming a Sprayable Nonisocyanate Polymer Foam Composition, CA2840738A1, 2014.

[25] O. Figovsky, L. Shapovalov, R. Potashnikov, Y. Tzaid, J. Bordado, D. Letnik, A. De Schijuer, Foamable Photo-Polymerized Composition US6960619 B2, 2005.

[26] O. Figovsky, L. Shapovalov, Preparation of Oligomeric Cyclocarbonates and their Use in Ionisocyanate or Hybrid Nonisocyanate Polyurethanes, WO2003028644 A2, 2003.

[27] H. Blattmann, M. Lauth, R. Mülhaupt, Flexible and Bio-Based Nonisocyanate Polyurethane (NIPU) Foams, Macromol. Mater. Eng. 301 (2016) 944–952, https://doi.org/10.1002/mame.201600141.

[28] F. Monie, B. Grignard, J.M. Thomassin, R. Mereau, T. Tassaing, C. Jerome, C. Detrembleur, Chemo- and Regioselective Additions of Nucleophiles to Cyclic Carbonates for the Preparation of Self-Blowing Non-Isocyanate Polyurethane Foams, Angew. Chem. – Int. Ed. 59 (2020) 17033–17041, https://doi.org/10.1002/anie.202006267.

[29] M.S. Hussein, T.P. Leng, A.R. Rahmat, F. Zainuddin, Y.C. Keat, K. Suppiah, Z. S. Alsagayar, The effect of sodium bicarbonate as blowing agent on the mechanical properties of epoxy, Mater. Today:. Proc. 16 (2019) 1622–1629, https://doi.org/10.1016/j.matpr.2019.06.027.

[30] ASTM D6226-21, Standard Test Method for Open Cell Content of Rigid Cellular Plastics, 2021. https://doi.org/10.1520/D6226-21.

[31] J. Pinto, E. Solórzano, M.A. Rodriguez-Perez, J.A. De Saja, Characterization of the cellular structure based on user-interactive image analysis procedures, J. Cell. Plast. 49 (2013) 555–575, https://doi.org/10.1177/0021955X13503847.